Reduction of electrical noise on diode trace measurements via a pulse replicator

Contact: pedro.oliveira@stfc.ac.uk

A. Mayouf, P. Oliveira
Central laser facility,
STFC Rutherford Appleton Laboratory
Harwell Campus
OXON. OX11 0QX, UK

Abstract

A low cost and easy to implement solution to increase the signal to noise ratio in single shot measurements is presented. Pulse replicas are created and redistributed to the same photodiode/oscilloscope combination. Averaging those replicas reduces the electrical noise in the pulse shape. We present simulation and experimental results including a calibration of the instrument.

Introduction

Averaging is a useful tool to increase the possible dynamic range of a measurement by increasing the signal to noise ratio [1]. On single shot systems it is not possible to average since there is only one measurement. Other works have used a bespoke fibre system that divides and recombines the beam using different path lengths. In this manner, the electrical noise endured by each pulse replica will be different therefore, averaging the different replicas minimises the electrical noise. Previous works imply needing to splice the fibre many times [2]. In this report we present an easy to implement and easy to use system that avoids any splicing and uses only off-the-shelf standard fibre elements whilst still producing pulse replicas with different electrical noise. We have tested in a proof-of-concept demonstration using one of our Shaped Long Pulse (SLP) systems in Vulcan. This is a simple 1053 nm laser, which works at 2 Hz. The technique of pulse replication averaging will be able to reduce electrical noise and allow us to evaluate whether or not we are in saturation on our detector. However, as the replications are parts of the original pulse, they cannot be used to eliminate other types of noise.

Pulse replicator concept

The fibre system will be used as a diagnostic tool without interfering with the results of the laser. The transmission of a mirror is aligned into a collimator connected to a 99% : 1% fibre splitter. This splitter is then connected to another similar fibre splitter, in the configuration shown in Figure 1. The two fibre splitters serve as a cavity where light gets trapped in the system. The pulse gets picked up at every turn of the fibre cavity in a 1% coupler and placed into the diagnostics. The diagnostics consist of a photodiode/ oscilloscope combination.

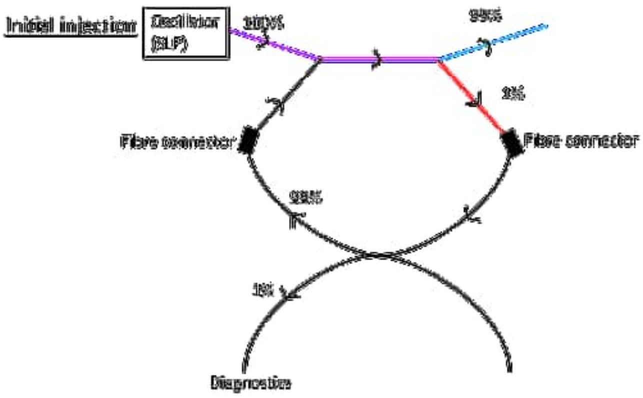

Figure 1: Fibre system setup showing initial injection from the oscillator into the two fibre splitters which had been connected together then into the diagnostics. The percentages of the intensity of light going through each section of the fibre system are shown.

Experimental setup

A schematic of the fibre system in Vulcan is shown in Figure 2.

One of the SLP systems from Vulcan was used to test the fibre system. A nanosecond pulse was used through the SLP. The transmission of a mirror was maximised by using a waveplate. In a full shot, the waveplate will not be needed as there will be enough leakage through a mirror at the end of the system, after the pulse is amplified.

Initial injection

In the initial injection, the pulse comes into the system with 100% going down one arm of the first fibre splitter. Taking the 1% output arm of this splitter to connect to another fibre splitter whilst the 99% output arm of the first splitter is dumped. Then taking the 1% output arm of the second splitter into the diagnostic setup whilst the 99% output arm of the second splitter is connected

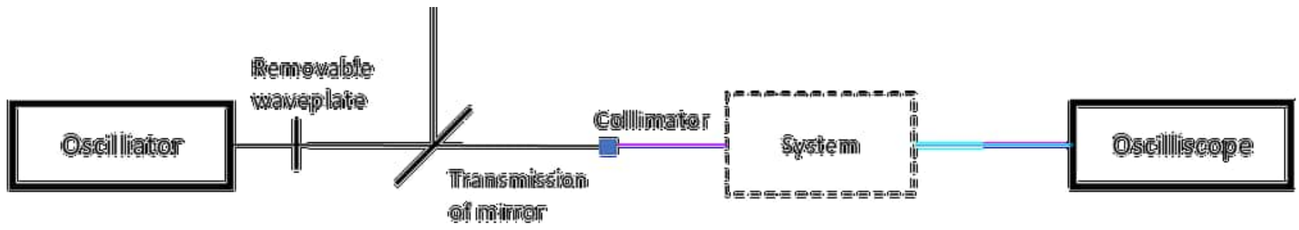

Figure 2: Schematic showing where the fibre system has been tested in Vulcan. The oscillator used here is the Shaped Long Pulse 3 and the path reflecting from the mirror goes to the rest of Vulcan to be amplified on a shot. The transmission of the mirror is taken into the fibre system for diagnostics which is shown as the oscilloscope. The removable waveplate is used before the mirror to increase the intensity of the transmitted light.

to the other arm of the input on the first splitter. The ratios of the splitters are shown in Figure 1.

Subsequent turns of the fibre cavity

In each turn after the initial injection, the pulse is now inputting through the other arm of the first splitter. This causes the ratio to be flipped on the output arms so that the 99% is taken into the second splitter and the 1% is dumped. The splitting ratio of the second splitter remains the same.

The limiting factor of the system is that the pulse duration cannot be more than the length of the fibre cavity, which was 8.4 ns here, otherwise the pulse replicas would interfere with themselves. However, a fibre patch cord can easily be added to increase the length of the fibre cavity.

Experimental results

We were able to replicate the pulse multiple times as shown in Figure 3. The repetitions also had an exponential decay since at every turn of the fibre cavity there would be a percentage loss of the previous signal intensity.

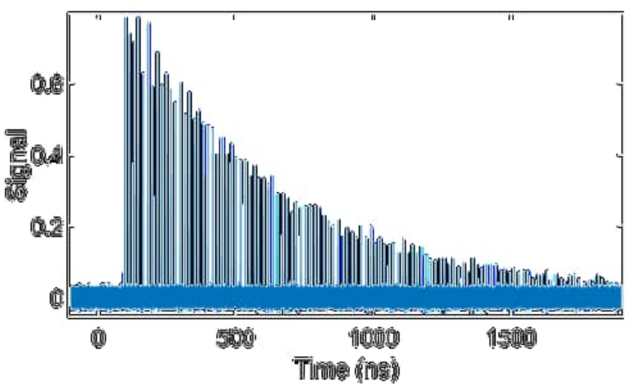

Figure 3: Exponential decay of signal over time.

System calibration

To calibrate our system, we must do two things: a time calibration and a characterisation of the loss. The time calibration is used to superimpose all the signals on top of each other. This is the equivalent of knowing the delay between the several replicas and will be intrinsic to the fibre cavity. The characterisation of the loss, l, between each pulse replica needs to be found for normalisation purposes. The results presented here are for a pulse with an obvious peak as it is important to calibrate the system with an easy to observe feature; but once the system is calibrated, it can be applied to other pulse shapes.

Time calibration

The pulse replicas should arrive at the diagnostics with approximately the same time difference between them, T, as seen in Figure 4, which is determined by the length of the fibre system. The peaks of the pulse replicas are found by using the $findpeaks$ function in Matlab. The average time difference between each pulse replica,T, can then be calculated by using

$$t_n = t_0 + nT, \tag{1}$$

where t_n is the time of the peak of the n^{th} pulse replica, t_0 is the time of the initial pulse replica, n is which number the pulse replica is.

After the time difference is found, it can be used to overlap the peaks of the pulse replicas so an average of the pulse shape can be found. The time difference can also be applied to different pulse shapes as long as the repetition rate is the same.

Characterisation of the loss

There is an exponential decay of the signal intensity of the pulse replicas for every turn of the fibre cavity which is shown in Figure 5. This is due to only taking 1% of the signal to the diagnostics each time. This means that before averaging, the pulses need to be normalised to counteract the loss.

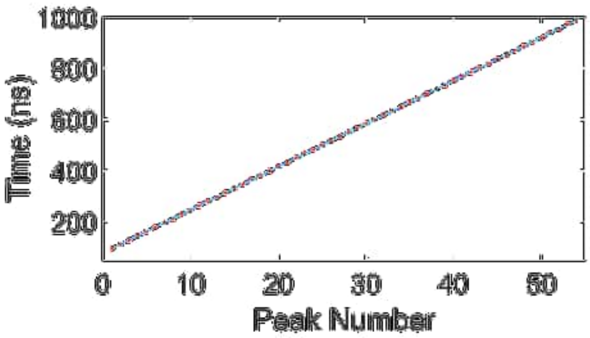

Figure 4: Blue line of best fit showing the time in nanoseconds against the peak number. The red dots show the time at which the peak of each pulse replica is recorded.

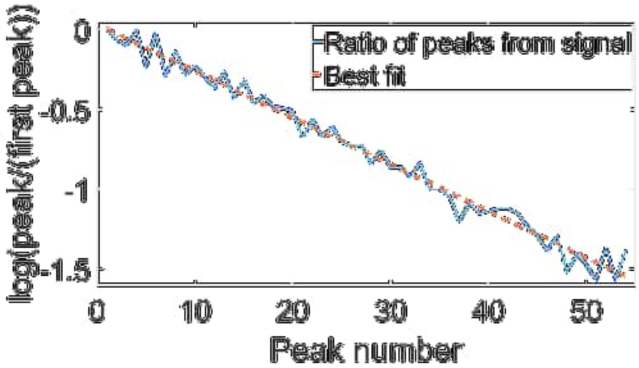

Figure 5: The blue line shows the relative intensity, $\log(\frac{\text{peak}}{\text{first peak}})$, of the peak of each pulse replica against the pulse replica number. The red dashed line is the line of best fit.

The intensity of each pulse replica can be modelled as

$$S_n = (1-l)^n S_0, \tag{2}$$

where S_n is the intensity of the n^{th} pulse replica, l is the loss in the pulse replica intensity per turn of the cavity, n is the pulse replica number and S_0 is the initial pulse replica intensity.

Using Equation 2 and rearranging into the form $y = mx$, as shown in Equation 3

$$\ln\left(\frac{S_n}{S_0}\right) = [\ln(1-l)]n, \tag{3}$$

in conjunction with Figure 5 finds the average loss to be 4.5% per turn of the fibre cavity. This is due to the splitters and the coupling between the fibres. The loss can then be used to normalise the pulse replicas by dividing each pulse repetition by $(1-l)^n$.

Noise analysis and discussion

The signal is normalised by multiplying the pulse replicas by $\frac{1}{(1-l)^n}$. This allows the pulse replicas to be averaged by putting the repetitions on top of each other and averaging point-by-point in time. Normalising also multiplies the electrical noise. The optimal number of pulse replicas used in the average is when the signal-to-noise ratio is the greatest. This is determined by taking the noise just after each pulse replica, normalising and averaging the noise over the number of replicas sampled then, taking the standard deviation of the averaged noise. The optimal is when the standard deviation of the noise is closest to zero, which is demonstrated in Figure 6. Averaging the normalised pulse replicas is representative of averaging over several identical measurements and is shown by the yellow line in Figure 6. The blue line shows what happens in our case where the signal magnitude decreases. The signal added at the start is much more than the noise. However, because of the signal-to-noise ratio, the signal added will decrease after each round trip in the fibre cavity. At some point when more noise is added than signal into the averaging, the benefits of averaging are negated. This gives the number of pulse replicas to use in the averaging. Here, the least noise in the signal is given when averaging 24 pulse replicas (please note, this is approximately $\frac{1}{4.5\%} = \frac{1}{\text{average loss}}$).

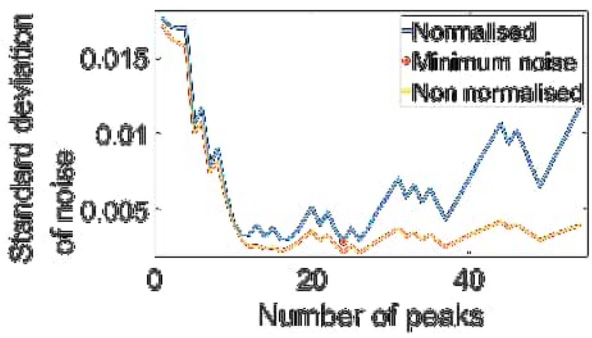

Figure 6: Top blue line is the normalised standard deviation of the averaged noise after each pulse replica against the number of pulse replicas averaged. Bottom orange line is the averaged standard deviation of the non-normalised noise against the number of pulse replicas averaged. The red dot on the blue line is the number of pulse replicas averaged to achieve the minimum noise (optimal).

After averaging over 24 pulse replicas, the signal to noise is increased by a factor of 7 which has been calculated by comparing the standard deviation of the noise before and after averaging. This allows the temporal pulse shape to be accurately measured as shown in the side-by-side comparison of no averaging and optimal averaging in Figure 7.

In Figure 6, it is notable that the standard deviation of the noise comes close to but, does not reach zero. This is due to other systematic errors that cannot be negated by averaging.

Another point of discussion is that increasing the sig-

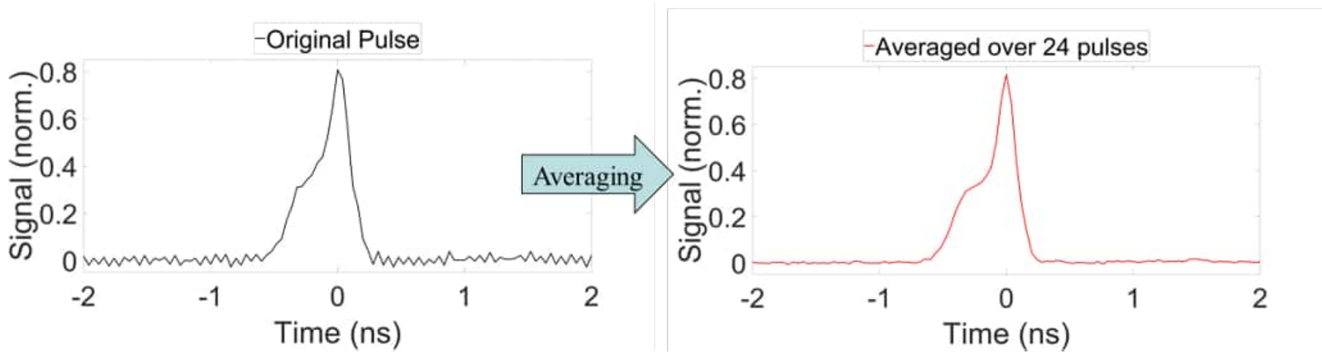

Figure 7: Pulse shape before averaging (left) compared with the pulse shape after optimal averaging (right).

nal increases the signal to noise ratio. However, this will also saturate the diode whereas this method can decrease the noise without reaching saturation.

Detector saturation

The detector being saturated causes the pulse replicas to remain the same height on the oscilloscope. This is a good way to tell if the photodiode is saturated. The method of averaging the pulse replicas can still be implemented after the pulse replicas decay enough that the exponential decay can be seen on the oscilloscope as this shows that the photodiode is no longer saturated and the pulse shape is now representative of the temporal pulse shape (albeit with noise). This is good as saturation and not knowing what filters to put on the system is not an issue (as long as the photodiode damage threshold is not exceeded).

Conclusion

We have demonstrated that simple off the shelf components allows us to increase the signal to noise by a factor of 7 in single shot systems. This uses two fibres coupled together and we should be able to implement it in the Vulcan laser system to accurately measure the temporal pulse shape and at the same time to be insensitive to saturation on the receptor since the analysis can chose other replicas to analyse. The system should have a significant impact operationally.

References

[1] U. Hassan and M. S. Anwar, "Reducing noise by repetition: introduction to signal averaging," *European Journal of Physics*, vol. 31, p. 453, mar 2010.

[2] C. Zhao, *Characteristics of Noise and Photon Statistics of Fiber Components in Electro-Optical Systems.* PhD thesis, 2013. Copyright - Database copyright ProQuest LLC; ProQuest does not claim copyright in the individual underlying works; Last updated - 2023-03-04.